Optics Communications 305 (2013) 17–22

Contents lists available at SciVerse ScienceDirect

Optics Communications

journal homepage: www.elsevier.com/locate/optcom

Discussion

Systematical research on the plasmon-induced transparency in coupled plasmonic resonators

Binfeng Yun, Guohua Hu, Yiping Cui *

Advanced Photonics Center, Southeast University, Nanjing 210096, China

ARTICLE INFO

Article history:
Received 20 February 2013
Received in revised form
13 April 2013
Accepted 24 April 2013
Available online 14 May 2013

Keywords:
Plasmon-induced transparency
Coupled Fabry–Perot
Plasmonic waveguide

ABSTRACT

The plasmon-induced transparency (PIT) realized in the coupled plasmonic resonators which are composed of the compact and detuned cavities is studied. By using the finite difference time domain (FDTD) method, the PIT system with coupled plasmonic Fabry–Perot (FP) resonators and coupled T-shaped plasmonic resonator are proposed and analyzed in detail; and the results show that the periodic electromagnetic-induced transparency can be realized which is determined by the detuning and destructive interference between the two coupled plasmonic resonators. Compared to the individual plasmonic resonator, the quality factor of the PIT peak is enhanced. Both the transmission enhancement and suppressing can be realized with the destructive and instructive interferences between the two coupled plasmonic resonators by adjusting the phase differences. Also a simple FP model is introduced to physically analyze the transmission characteristics of the system, and the results are well correlated with the FDTD method. The proposed compact PIT waveguides are very promising for nanoscale optical filtering and slow light devices in high-density plasmonic waveguide integrations.

1. Introduction

Surface plasmon polaritons (SPP) are electromagnetic waves coherently coupled to electron oscillations and propagating at the interface between a dielectric and a conductor, with evanescently decaying fields in both sides [1]. The metal/insulator/metal (MIM) SPP waveguide is a very promising nanoscale waveguide which can overcome the diffraction limit in conventional dielectric waveguide. Some nanometric filters based on the MIM waveguides have been proposed, such as the ring resonator filters [2–4], cavity resonator filters [5], tooth-shaped filters [6,7], Bragg grating filters [8,9], Fabry–Perot filters [10,11]. Electromagnetically induced transparency (EIT) is a phenomenon occurs in atomic systems as a result of quantum interference between the atomic levels and the applied laser [12]; and several optical analogues of EIT configurations with dielectric waveguides have been observed and analyzed [13,14]. Recently, a number of compact PIT configurations which are plasmonic analogue of the EIT have been proposed, such as the metal nano-antenna coupled dielectric waveguide [15] and the coupled plasmonic resonators [16–19]; and in all these systems, the detuning between the coupled resonators is one of the key points to realize the PIT. However, for the metal nano-antenna coupled dielectric waveguide system [15], the transmission ratio is relative low because of the high damping rate of the metal nano antenna. While for the PIT systems which are composed of detuned plasmonic resonators [18,19], only the situation with zero phase difference between the detuned resonators are considered and analyzed; and Han et al. briefly mentioned that the PIT spectrum was deteriorated by introducing small phase difference between the detuned resonators and cannot be gained [18]. But actually the PIT spectrum is very sensitive to the phase difference between the detuned resonators and can be modulated periodically according to the destructive and instructive interferences, which has not been analyzed. Recently two identical plasmonic resonators (without detuning) with the phase differences between them are introduced to enhance the filter transmission [20] or rejection [21], but they are not the PIT system and their bandwidths are much larger than those of the PIT system. So in a word, the PIT is related to the phase difference between the detuned resonators, and the corresponding physics needs to be clarified. In this article, the effects of phase differences between two detuned plasmonic resonators are analyzed, and the corresponding PIT characteristics are studied. By using the FDTD method, the transmission characteristics of the PIT systems composed of detuned resonators with phase difference between them are analyzed in detail. The results show that both the transmission enhancement and suppression in the PIT system according to the destructive and instructive interferences respectively can be realized by adjusting the phase differences. Also a simple FP model is introduced to physically analyze the transmission spectra of the coupled plasmonic FP and T-shaped resonators, which correlates the FDTD results very well. The simple FP model

* Corresponding author. Tel.: +86 25 83792470 x8208; fax: +86 25 83790201.
E-mail address: cyp@seu.edu.cn (Y. Cui).

0030-4018/$ - see front matter © 2013 Elsevier B.V. All rights reserved.
http://dx.doi.org/10.1016/j.optcom.2013.04.064

is universal and can be used in other plasmonic PIT systems that are composed of two detuned resonators.

2. PIT in coupled plasmonic FP resonator system

The schematic of the proposed PIT system with two detuned plasmonic FP resonators is shown in Fig. 1(a). L_1, L_2, d are the lengths of the two detuned FP resonators and the distance between them, and $w=100$ nm, $g=10$ nm are the width of the MIM waveguide and the gap between the FP resonator and the input MIM waveguide. The total structure is base on the nano-metric MIM plasmonic waveguide, and the dispersion relation of the fundamental TM mode in the MIM waveguide is given by [6]

$$\varepsilon_{in}k_{z2}+\varepsilon_m k_{z1}\coth\left(-\frac{ik_{z1}}{2}w\right)=0 \tag{1}$$

and k_{z1} and k_{z2} are

$$k_{z1}^2=\varepsilon_{in}k_0^2-\beta^2,\quad k_{z2}^2=\varepsilon_m k_0^2-\beta^2 \tag{2}$$

where ε_{in} ,ε_m are the dielectric constants of the insulator and the metal,$k_0=2\pi/\lambda$ is the free-space wave vector, and the dielectric constant of the metal silver is characterized by the Drude model [6,16]

$$\varepsilon_m(\omega)=\varepsilon_\infty-\omega_p^2/\omega(\omega+i\omega) \tag{3}$$

where $\varepsilon_\infty=1.38\times10^{16}$ Hz is the bulk plasma frequency, which represents the nature frequency of the oscillations of free conduction electrons; $\gamma=2.73\times10^{13}$ Hz is the damping frequency of the oscillations, ω is the angular frequency of the incident light, and $\varepsilon_\infty=3.7$ is the dielectric constant at infinite angular frequency [6,16]. The real part of the effective index of the fundamental TM mode ($n_{\text{eff}}=\beta/k_0$) as a function of slit width w and incident light wavelength λ is shown in Fig. 1(b). The n_{eff} decreases as d increases and decreases relatively slow with increasing λ.

The 2D FDTD method with perfect matched layer boundary condition is used to simulate the transmission spectra of the PIT systems. The fundamental TM mode of the MIM waveguide is excited by a dipole source, and the mesh grid size is set to 1 nm in order to keep convergence. Two monitors PD1 and PD2 are set to detect the incident power A_1 (without the coupled resonators for reference) and the transmission power A_2 (with the coupled resonators). The transmittance is defined as $T=A_2/A_1$[4,6].

Two detuned plasmonic FP resonators with length L_1=500 nm and L_2=480 nm are used to construct the plasmonic PIT system, and their corresponding transmission spectra are simulated by the FDTD method and shown in Fig. 2(a). The two resonance dips of the detuned FP resonantors are at 677 nm and 700 nm which are the 2nd-order (N=2) resonances [10] of the FP resonators from the H_y field distribution shown in the inset of Fig. 2(a). Also the transmission spectrum of the plasmonic PIT system which includes the two FP resonators separated by $d=280$ nm is shown in Fig. 2(a) for comparison. It is obvious that there is an enhanced transmission window at 689 nm which is caused by the plasmonic analogue of the PIT effect. The quality factor of the PIT peak is

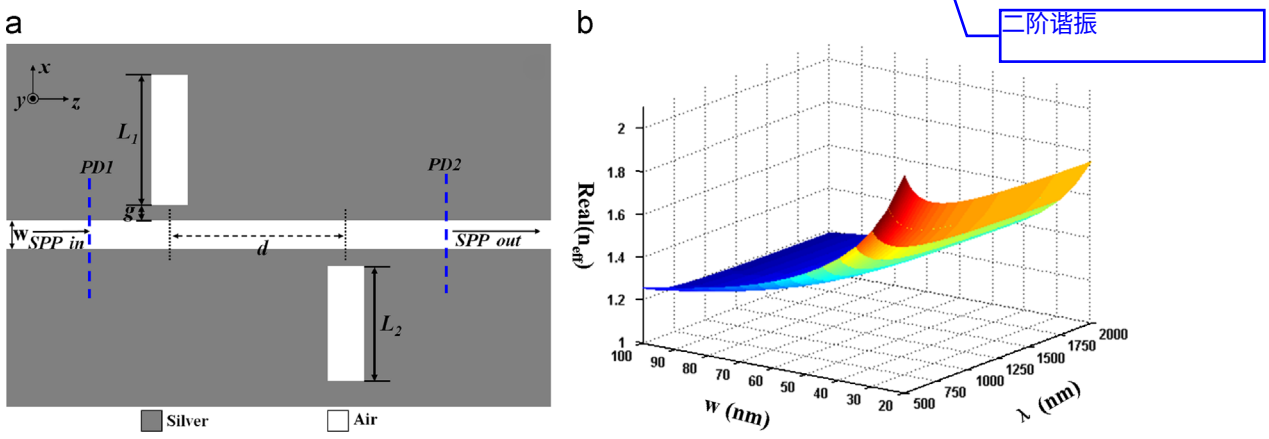

Fig. 1. (a) The PIT waveguide composed of two detuned plasmonic FP resonators. (b) The dependence of Re(n_{eff}) of the fundamental TM mode on the wavelength of incident light λ and the width w.

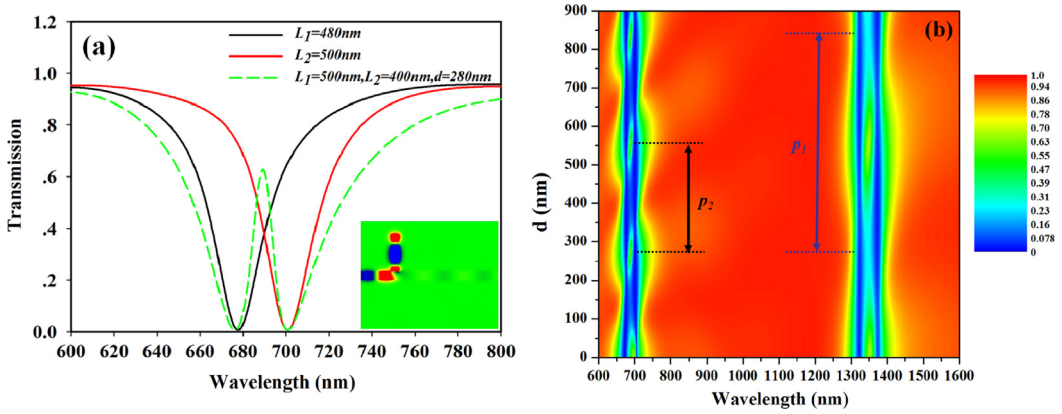

Fig. 2. (a) The transmission spectra of the two detuned plasmonic FP resonators and the corresponding PIT waveguide constructed by them ($L_1=500$ nm, $L_2=480$ nm, $d=280$ nm). The inset shows the H_y field distribution of the resonant mode. (b) The contour plot of the transmission spectra with different distance d between two FP resonators.

Q_{PIT}≈76, which is about three times of the isolated FP resonator (Q_1≈25 and Q_2≈24). This quality factor enhancement effect is the one of the characteristics of the PIT in plasmonic waveguide [18] and is very promising for the plasmonic wavelength filtering and demultiplexing [17]. In order to investigate the effect of the phase difference between the two coupled plasmonic FP resonators, the distance d was adjusted from 0 nm to 900 nm and the corresponding contour plot of the transmission spectra is shown in Fig. 2(b). In Fig. 2(b) two groups of PIT peaks can be observed: The PIT peaks at around λ_1≈1350 nm are caused by the interferences of the 1st-order FP resonance modes, and the PIT peaks at around λ_2≈690 nm are the results of the 2nd-order FP resonance coupling. The small discrepancy with $\lambda_1=2\lambda_2$ is due to the MIM waveguide dispersion as shown in Fig. 1(b). From Fig. 2(b), it is obvious that the PIT peak transmission ratios are affected by the distance d between the two coupled plasmonic FP resonators, and a periodic PIT pattern is formed. The periods for the PIT caused by the 1st- and 2nd-order FP resonances coupling are about $p_1=560$ nm and $p_2=280$ nm, respectively. In Fig. 2(b), not only the transmission enhancement of PIT can be realized, but also the transmission suppression can be introduced. In order to physically analyzing the transmission enhancement and suppression effects, the two detuned plasmonic FP resonators can be regarded as frequency dependent partly reflectors and the whole PIT system can be modeled as another FP resonator with a cavity length of d. Then the transmission of the PIT system can be expressed as [15]

$$T_{EIT}(\lambda)=\left|\frac{t_1(\lambda)t_2(\lambda)}{1-r_1(\lambda)r_2(\lambda)e^{i2\beta(\lambda)d}}\right|^2 \quad (4)$$

where $r_{1,2}(\lambda)$ and $t_{1,2}(\lambda)$ are the frequency-dependent reflection (transmission) coefficients of the two detuned plasmonic FP resonators, and $\beta=2\pi n_{eff}/\lambda$ is the propagation constant of the MIM waveguide mode and n_{eff} is the effective index of the MIM waveguide mode.

The transmission spectra of the coupled plasmonic FP resonator systems simulated by the numerical FDTD method (solid line) and the analytic FP model (dash line) are shown in Fig. 3. Both the 1st- and 2nd-order FP resonances coupling can induce the transmission enhancement and suppression depending on the distance d between the two detuned FP resonators. When $d=0$ nm, both the 1st- and 2nd-order FP resonance coupling can induce the transmission enhancement (i.e. PIT); when $d=280$ nm, the 1st-order FP coupling induces PIT while the 2nd-order FP coupling introduces the transmission suppression; when $d=400$ nm, both the 1st- and 2nd-order FP coupling cause the transmission suppression; when $d=560$ nm, both the 1st- and 2nd-order FP couplings induce the PIT. The transmission suppression in the coupled plasmonic FP resonator system can induce a broader stop band compared with that of the individual FP resonator, and can be used as a broad band-stop filter. So as can be concluded from Fig. 2(b), the PIT appears when $d=n\times p_{1(2)}$ (n=0,1,2…), while the transmission suppression happens when $d=(n+1/2)\times p_{1(2)}$(n=0,1,2…). According to the phase match condition of the FP model in Eq.(4), the maximum and minimum transmissions can be obtained when $d=n\lambda_{neff}/2$ and $d=(n/2+1/4)\lambda_{neff}$ are satisfied, respectively. So the period $p_{1(2)}=\lambda_{neff1(2)}/2$, where λ_{neff} is the effective plasmonic wavelength of the MIM waveguide. According to the MIM waveguide dispersion relation (1), half of the effective plasmonic wavelengths at the 1st (1350 nm) and 2nd (690 nm) resonances are $\lambda_{neff1}/2=565$ nm and $\lambda_{neff2}/2=283.5$ nm, respectively, which match the periods obtained by the FDTD method $p_1=560$ nm and $p_2=280$ nm well. This is also confirmed in the H_y field distributions of the coupled plasmonic FP resonator systems as shown in Figs. 4 and 5. It is obvious that when $d=p_1=280$ nm, the H_y field in the MIM waveguide between the

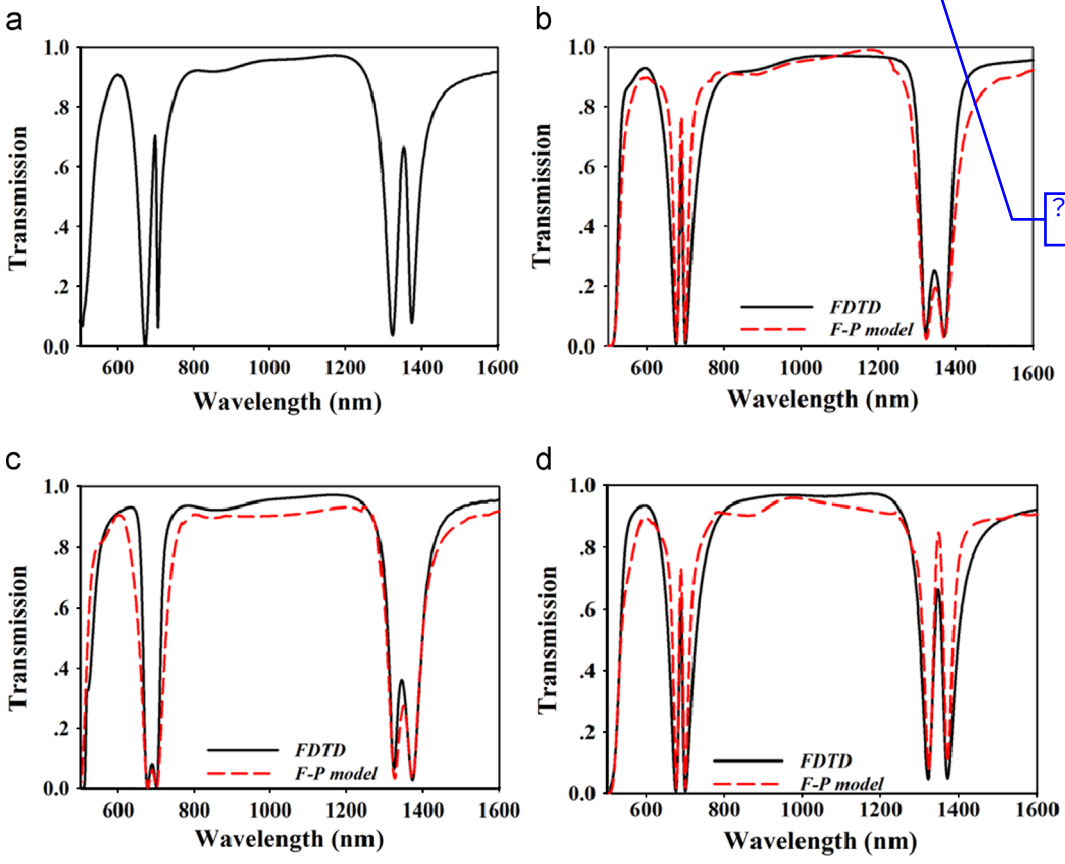

Fig. 3. The transmission spectra of the PIT system with coupled plasmonic FP resonators (solid lines are the FDTD results and the dash lines are the FP model results). (a) d=0 nm; (b) d=280 nm; (c) d=400 nm; (d) d=560 nm.

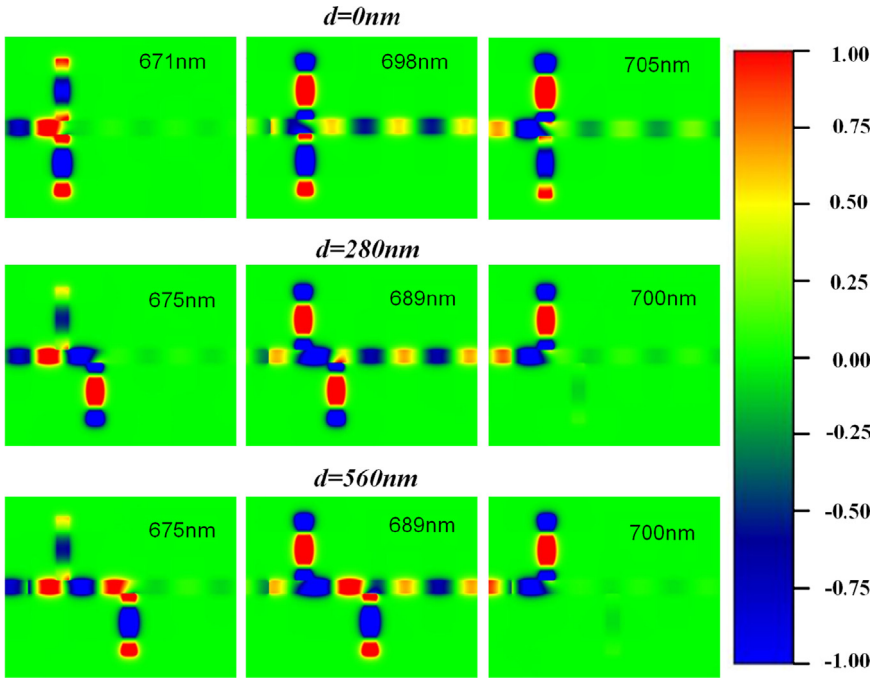

Fig. 4. The H_y field distributions at the transmission dips and PIT peaks of the 2nd-order FP modes coupling in the coupled plasmonic FP resonator system.

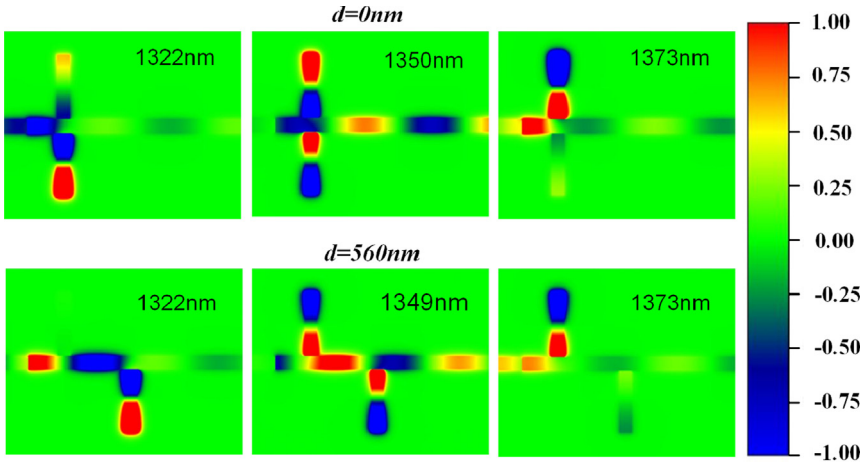

Fig. 5. The H_y field distributions at the transmission dips and PIT peaks of the 1st-order FP modes coupling in the coupled plasmonic FP resonator system.

two detuned plasmonic resonators shows a half wavelength pattern, while when $d = 2 \times p_1 = 560$ nm, the H_y field shows an one wavelength pattern. This pattern can also be seen in the 1st-order FP modes coupling in Fig. 5. It should be noted that the 2nd resonance modes in the two detuned FP resonators are antiphase when $d = 0$ nm, which induce the destructive interference and cause the PIT effect as same as the result in Ref. [18]. But from Figs. 4 and 5, the conclusions in Ref. 18 is not complete because when $d = \lambda_{neff}/2$, the resonance modes in the two detuned FP resonators are in phase and can also induce the PIT effect. In conclusion, the resonance modes in the two detuned FP resonators are antiphase when $d = n \times \lambda_{neff}$ $(n = 0,1,2,\ldots)$ and inphase when $d = (n + 1/2) \times \lambda_{neff}$ $(n = 0,1,2,\ldots)$ both can induce the destructive interference between the two detuned FP resonators. And when the destructive interference condition reached, the transmission of the coupled system is enhanced and the PIT effect appears. As also shown in Figs. 4 and 5, when incident wavelength equal to either resonance wavelength of the two detuned FP resonators, the incident light mainly resonants in that corresponding FP resonator, which acts as a bandstop filter.

3. PIT in coupled T-shaped plasmonic resonator system

For the proposed PIT system composed two coupled plasmonic FP filters above, the gap g is kept at 10 nm to get enough coupling between the FP cavities and the input MIM waveguide, which is relative difficult for the fabrication. In order to increase the coupling and make it easy for fabrication, a PIT system composed of two detuned plasmonic T-shaped resonators is proposed and shown in Fig. 6. Here $w = 50$ nm and $h = 100$ nm are the MIM waveguide width and the vertical coupling parts of the T-shaped resonator, respectively.

Also the phase difference between the two coupled plasmonic T-shaped resonators is adjusted by changing the distance d from 0 nm to 600 nm and the corresponding contour plot of the transmission spectra are shown in Fig. 7(a). Again periodic transmission enhancement and suppression patterns are shown due to the destructive and instructive interferences between the two coupled T-shaped plasmonic resonators. The period $p = 280$ nm approximately satisfies the phase match condition of the destructive interference at the PIT

peak wavelength $\lambda = 748$ nm ($p = \lambda_{neff}/2 \approx 270$ nm). In order to investigate the resonator detuning effect on the PIT, the cavity length of one coupled T-shaped resonator is kept at $L_1 = 500$ nm while the cavity length of the another T-shaped resonator L_2 is changed. Fig. 7 (b–d) shows the transmission contour plots of the coupled T-shaped plasmonic resonator systems with $L_2 = 540$ nm, 560 nm and 580 nm. It is obvious that the transmission ratio at the PIT peak is enhanced when the detuning increases, which is consisted with the plasmonic nanoantenna coupled PIT system [15].

The transmission spectra of the PIT system with coupled plasmonic T-shaped resonators obtained by the numerical FDTD method and the analytic FP model are compared as shown in Fig. 8. The results show that both the transmission enhancement and suppression effect can be well analyzed by the simple FP model.

The H_y fields at the transmission dips and the PIT peak with $d = 0$ nm and $d = 280$ nm are shown in Fig. 9. Similar to the coupled plasmonic FP system, when $d = 0$ nm, the resonances in the two coupled T-shaped plasmonic resonators are antiphase, while inphase when $d = 280$ nm. Both of them can induce the destructive interferences which cause the PIT phenomenon. Also when incident wavelength is equal to either resonance wavelength of the two detuned T-shaped resonators, the incident light mainly resonants in that corresponding T-shaped resonator, which acts as a bandstop filter.

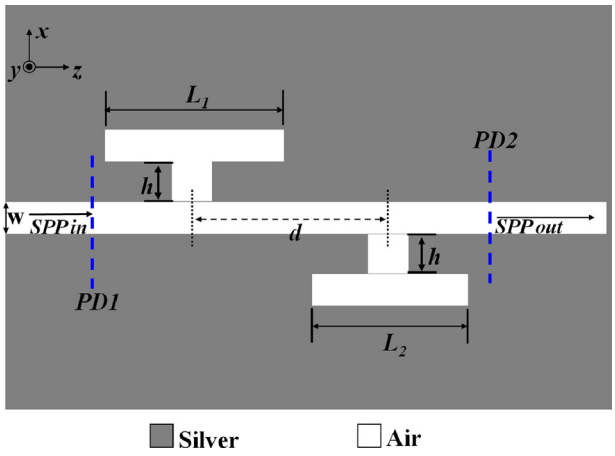

Fig. 6. The PIT waveguide composed of two detuned plasmonic T-shaped resonators.

4. Conclusion

In this article, the plasmon-induced transparency in coupled plasmonic resonators is investigated, and two typical PIT configurations are presented and analyzed in detail. Both the coupled plasmonic FP and T-shaped plasmonic resonators show PIT effects when the destructive interferences between them are introduced. Also both the transmission enhancement (PIT) and suppression effects show a periodic behavior because of the periodic interference

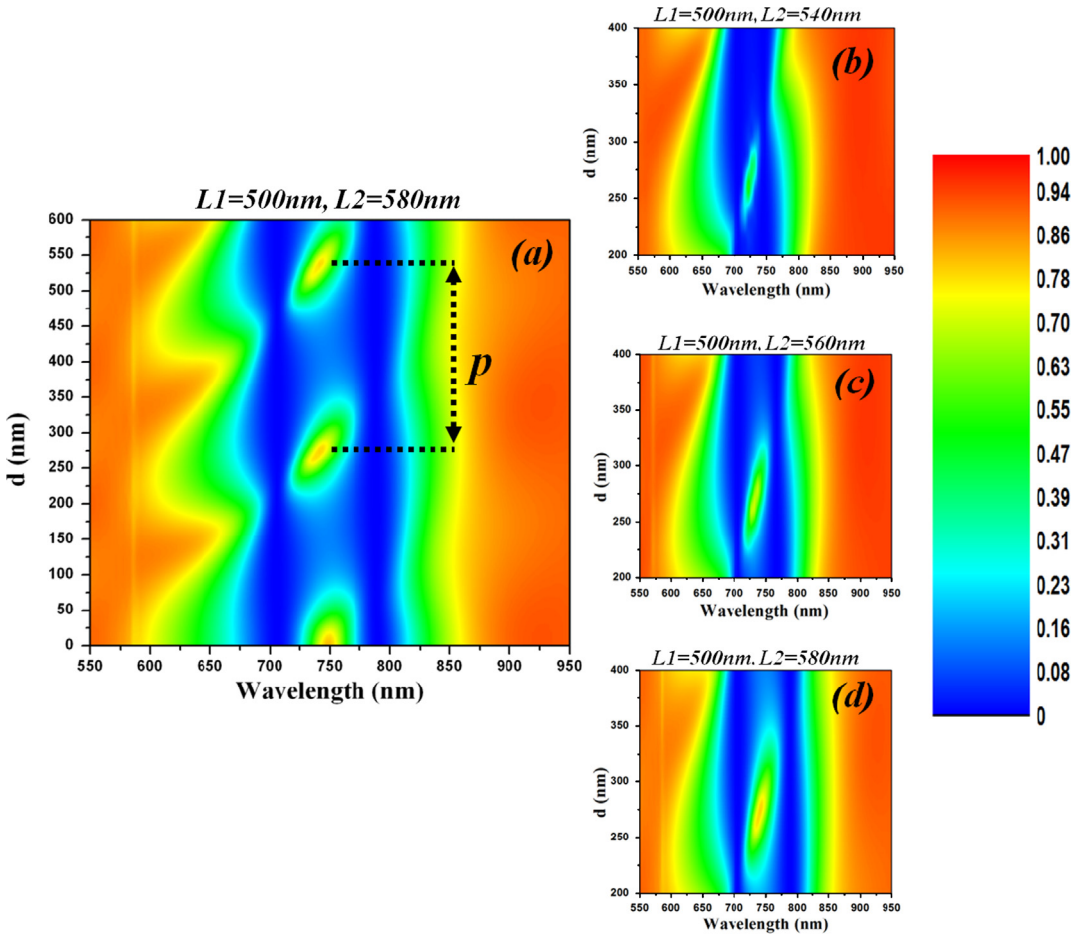

Fig. 7. The contour plots of the transmission spectra with different distance d between two T resonators ($w = 50$ nm, $h = 100$ nm). (a and d) $L_1 = 500$ nm, $L_2 = 580$ nm; (b) $L_1 = 500$ nm, $L_2 = 540$ nm; (c) $L_1 = 500$ nm, $L_2 = 560$ nm.

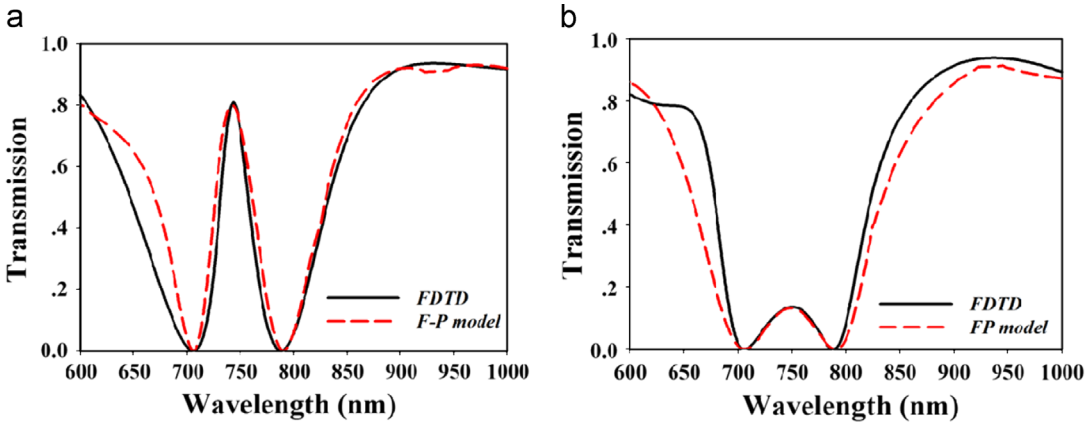

Fig. 8. The transmission spectra of the PIT system with coupled plasmonic T shaped resonators (solid lines are the FDTD results and the dash lines are the FP model results). (a) $d=280$ nm; (b) $d=400$ nm.

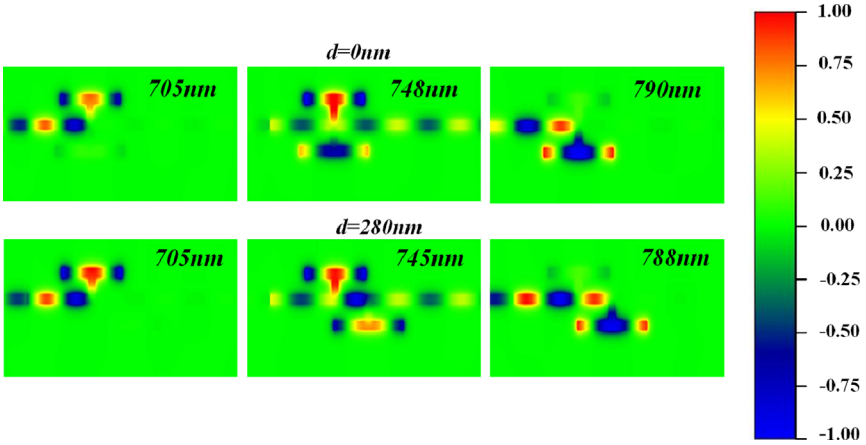

Fig. 9. The H_y field distributions at the transmission dips and PIT peaks of the coupled plasmonic T shaped resonator system.

patterns, which is determined by the phase difference between the two coupled plasmonic resonators. The transmission peak valued of the PIT system can be enhanced by increasing the detuning of the coupled plasmonic resonators. A simple analytic FP model is introduced to analyze the PIT system responses physically, and the obtained results correlate to the numerical FDTD results well. The simple FP model can be used in other kinds of PIT systems which includes two coupled plasmonic resonators.

Acknowledgments

This work was supported by the National Science Foundation of China under Grant No.60907025 and Science Foundation of Southeast University under Grant No. KJ2009358.

References

[1] Ekmel Ozbay, Science 311 (2006) 189.
[2] Sanshui Xiao, Liu Liu, Min Qiu, Optics Express 14 (2006) 2932.
[3] Amir Hosseini, Yehia Massoud, Applied Physics Letters 90 (2007) 181102.
[4] Binfeng Yun, Guohua Hu, Yiping Cui, Journal of Physics D: Applied Physics 43 (2010) 385102.
[5] Binfeng Yun, Guohua Hu, Yiping Cui, Plasmonics (2012), http://dx.doi.org/10.1007/s11468-012-9384-y.
[6] Xian-Shi Lin, Xu-Guang Huang, Optics Letters 33 (2008) 2874.
[7] Jin Tao, Xuguang Huang, Xianshi Lin, Jihuan Chen, Qin Zhang, Xiaopin Jin, Journal of the Optical Society of America B: Optical Physics 27 (2010) 323.
[8] Amir Hosseini, Hamid Nejati, Yehia Massoud, Optics Express 16 (2008) 1475.
[9] Yongkang Gong, Leiran Wang, Xiaohong Hu, Xiaohui Li, Xueming Liu, Optics Express 17 (2009) 13727.
[10] Binfeng yun, Guohua Hu, Yiping Cui, Optics Communications 284 (2011) 485.
[11] Lin Liu, Xia Hao, Yutang Ye, Juanxiu Liu, Zhenlong Chen, Yuncen Song, Ying Luo, Jing Zhang, Liang Tan, Optics Communications 285 (2012) 2558.
[12] M. Fleischhauer, A. Imamoglu, J.P. Marangos, Reviews of Modern Physics 77 (2005) 663.
[13] Edo Waks, Jelena Vuckovic, Physical Review Letters 96 (2006) 153601.
[14] Qianfan Xu, Sunil Sandhu, Michelle L. Povinelli, Jagat Shakya, Shanhui Fan, Michal Lipson, Physical Review Letters 96 (2006) 123901.
[15] Rohan D. Kekatpure, Edward S. Barnard, Wenshan Cai, Mark L. Brongersma, Physical Review Letters 104 (2010) 243902.
[16] Hua Lu, Xueming Liu, Dong Mao, Yongkang Gong, Guoxi Wang, Optics Letters 36 (2011) 3233.
[17] Jianjun Chen, Zhi Li, Jia Li, Qihuang Gong, Optics Express 19 (2011) 9976.
[18] Zhanghua Han, Sergey I. Bozhevolnyi, Optics Express 19 (2011) 3251.
[19] Yin Huang, Changjun Min, Georgios Veronis, Applied Physics Letters 99 (2011) 143117.
[20] Hua Lu, Xueming Liu, Yongkang Gong, Dong Mao, Leiran Wang, Optics Express 19 (2011) 12885.
[21] Qiaodong Huang, Ruisheng Liang, Pixin Chen, Shun Wang, Yi Xu, Journal of the Optical Society of America B: Optical Physics 28 (2011) 1851.